Section: Radiodiagnosis

Original Research Article

A STUDY ON MRI EVALUATION OF SELLAR AND PARASELLAR MASS LESIONS WITH CLINICOPATHOLOGICAL CORRELATION IN A TERTIARY CARE TEACHING HOSPITAL

Dhruva Rajgopal[1], Bharat MP[2]

[1]Associate professor, Department of Radiodiagnosis, Siddaganga Medical College and Research Institute, Tumkur, Karnataka, India.
[2]Professor, Department of Radiodiagnosis, Subbiah Institute of Medical Sciences, Shivamogga, Karnataka, India.

Received : 01/03/2024
Received in revised form : 12/05/2024
Accepted : 28/05/2024

Keywords:
MRI sellar lesions, MRI para sellar Lesions, MRI adenoma, Dural Tail Sign, Cavernous sinus invasion.

Corresponding Author:
Dr. Bharat M P,
Email: mpbharat80@gmail.com

DOI: 10.47009/jamp.2024.6.3.50

Source of Support: Nil,
Conflict of Interest: None declared

Int J Acad Med Pharm
2024; 6 (3); 234-241

Abstract

Background: The sellar and parasellar region is an anatomically complex area that serves as a critical crossroads for critical neurovascular structures such as the orbits, cavernous sinus and its contents, suprasellar cistern and its contents, circle of Willis, hypothalamus via the pituitary stalk, and dural reflections forming the diaphragm sellae and cavernous sinuses. The aim is to correlate diagnosis on Magnetic Resonance Imaging with Pathological diagnosis. The objective is to describe the demographics of sellar and para sellar lesions, to determine the sensitivity, specificity, positive predictive value, negative value, and accuracy of MRI in diagnosing various sellar and parasellar lesions. **Materials and Methods:** Study Design a prospective hospital-based observational study. Study area is Department of Radio Diagnosis, in a tertiary care teaching hospital. Study Period is 1 year. Study population is patients who were referred to the Department of Radiodiagnosis for MRI brain/sella, with varying presentations, and suspicious of sellar and para sellar masses were included in the study. Sample size study consisted of 30 subjects. Sampling method simple random technique. Study tools and Data collection procedure; Material used- in all studies, MR imaging was performed with a clinical 1.5 T system (General electrical medical systems). A Brain Coil was used. A total of 30 patients who were referred to the Department of Radiodiagnosis for MRI brain/sella, with varying presentations, and suspicions of sellar and para sellar masses were included in the study after informed consent. In all patients, complaints, history, clinical examination, other investigations and clinical diagnosis were obtained. The histopathological report was obtained from those who were operated on. The radiological diagnosis was correlated with clinical and histopathological diagnosis. **Result:** The sensitivity of MRI diagnosis of Craniopharyngioma compared with histopathology is 75% and its specificity is 92.8%. The positive predictive value for MRI diagnosis of Craniopharyngioma compared with histopathology is 75% and its Negative predictive value is 92.8%. The per cent agreement for comparison of MRI diagnosis of Craniopharyngioma compared with histopathology is 88.9% and positive per cent agreement is 75%. When kappa statistics is applied the kappa value is 0.679, this shows substantial agreement between the MRI Diagnosis and Histopathological diagnosis of Macroadenoma with the statistically significant p-value of 0.004. **Conclusion:** The MR imaging properties of the four most prevalent lesions were distinct enough to distinguish them from one other and the majority of other entities. Other imaging characteristics, such as augmentation post-contrast, the presence of cystic components, extracellular and intrasellar placement, and clinical complaints, allow for additional separation among the various other abnormalities. MR imaging's better resolution and multiplanar capability best display the extent of sellar and parasellar lesions.

INTRODUCTION

The sellar and parasellar region is an anatomically complex area that serves as a critical crossroads for critical neurovascular structures such as the orbits, cavernous sinus and its contents, suprasellar cistern and its contents, circle of Willis, hypothalamus via the pituitary stalk, and dural reflections forming the diaphragm sellae and cavernous sinuses. The cavernous sinus is the most important parasellar structure, however, other structures that surround the sella turcica are included in the parasellar region from a practical and clinical standpoint. The anatomy of the sellar and parasellar regions is complex, with a wide range of diseases.[1]

The sella contains a variety of tumours, cysts, vascular lesions, inflammatory processes, infections, and congenital lesions. The clinical manifestation of sellar and parasellar lesions varies. Some of the most prevalent symptoms are pituitary axis failure, visual field abnormalities, hydrocephalus, intracranial mass effect, and other neurologic impairments.[2,3]

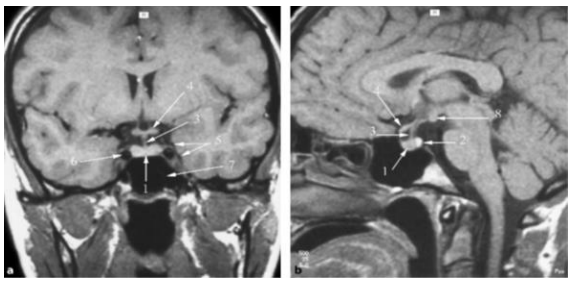

Figure 1: MR Coronal(a) and mid-sagittal (b) T1 images showing pituitary gland and para sellar area.1 Adenohypophysis, 2neurohypophysis, 3 infundibulum, 4 optic chiasm, 5 cavernous sinus, 6 intracavernous segments of the internal carotid artery, 7sphenoidal sinus, 8 mamillary bodies

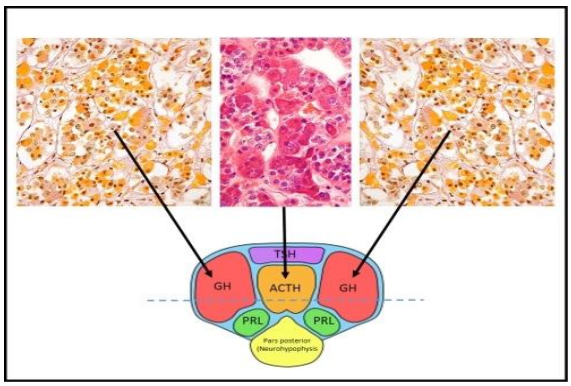

Figure 2: Axial section of the anterior lobe of the human pituitary gland (adenohypophysis) at the level indicated by the dashed blue line in the diagram. Although there is a mixture of different hormone-producing cells in most pituitary acini, the distribution of cells is not random: this is most pronounced in the 'lateral wings', which contain mostly somatotroph cells and the central 'mucoid wedge', which contains the majority of the corticotrophs. This is easily appreciated in periodic acid-Schiff / orange-G (PAS-OG) histochemistry, which stains somatotrophs yellow-orange (OG-positive) and corticotrophs purple (PAS-positive).

Although various imaging modalities are used to assess this area, the introduction and widespread use of high-resolution computed tomography (CT) has rendered its imaging forerunners, such as plain skull roentgenograms, pleuridirectional tomography, and pneumoencephalography, obsolete.[4]

Magnetic resonance imaging (MRI) is now widely available, and a substantial body of experience in using it to examine this region has been developed. MRI is now universally acknowledged as the imaging technique of choice for assessing sellar and parasellar pathology. Its main advantages are its improved soft tissue contrast and multiplanar imaging capability. There is no bone artefact, and the patient is not subjected to ionizing radiation. MRI can detect the involvement of the optic chiasm, cavernous sinus, sphenoid sinus, orbit, temporal lobes, and carotid arteries.[5]

CT is the recommended imaging modality for assessing calcification and bone detail. CT, on the other hand, has its limitations, including high doses of ionizing radiation, artefacts caused by the presence of bony structures, and the intrinsic limits of soft tissue resolution. However, CT remains an important screening method. Regardless of the imaging modality utilized, reviewing normal radiological anatomy and surveying the more common types of pathologic entities that develop in it is beneficial.[6-8]

Aim: To correlate diagnosis on Magnetic Resonance Imaging with Pathological diagnosis.

Objectives:

1. to describe the demographics of sellar and para-sellar lesions
2. to determine the sensitivity, specificity, positive predictive value, negative value, and accuracy of MRI in diagnosing various sellar and parasellar lesions.

MATERIALS AND METHODS

Study Design: A prospective hospital-based observational study.

Study area: Department of Radiodiagnosis, in a tertiary care teaching.

Study Period: 1 year.

Study population: Patients who were referred to the Department of Radiodiagnosis for MRI brain/sella, with varying presentations, and suspicious of sellar and para sellar masses were included in the study.

Sample size: The study consisted of 30 subjects.

Sampling method: Simple random technique.

Inclusion criteria

- Consent.
- Presenting with sellar and parasellar clinical features.
- Age 5-80years.

Exclusion criteria

- Previously diagnosed with pathologies in the area of interest and

ISSN (O): 2687-5365; ISSN (P): 2753-6556

- With renal diseases contraindicating contrast studies
- Patients with ferromagnetic substances e.g., pacemakers
- Claustrophobic patients.

Ethical Consideration: Institutional Ethical committee permission was taken before the commencement of the study.

Study tools and Data collection procedure: Material used: In all studies, MR imaging was performed with a clinical 1.5 T system (General electrical medical systems). A Brain Coil was used. A total of 30 patients who were referred to the Department of Radiodiagnosis for MRI brain/sella, with varying presentations, and suspicions of sellar and para sellar masses were included in the study after informed consent. In all patients, complaints, history, clinical examination, other investigations and clinical diagnosis were obtained. The histopathological report was obtained from those who were operated on. The radiological diagnosis was correlated with clinical and histopathological diagnosis.

Sequences

1. Axial, coronal and sagittal T2-weighted FSE with TR/TE 4800/80 to 90millisecs, Field of view 24 x 24cm, Matrix size 512 x 512 slice thickness 3mm, interslice gap 1.5mm, NEX (No. Of Excitations) 1.
2. Axial T1 with TR /TE 540/16 millisecs, Field of view 24 x 24cm, Matrix 512 x 512 slice thickness 3mm, interslice gap 1.5mm.
3. Spoiled gradient recalled TR/TE17-25/3-5, flip angle 35 degrees, fov 22x22cm, slice thickness 2mm.no interslice gap, Matrix size 512 x 512NEX (No. Of Excitations) 1.
4. Dynamic Gd-enhanced MR imaging using T1 coronals, delayed sagittal and axials were taken. The time of imaging was kept identical.
5. DWI: Field of view 26cm, Slice thickness 5mm with interslice gap of 1.5mm, number of excitations (NEX) = 3, matrix size 128×128, TR/TE 1000/81, B value 1000.
6. A power injector was used for the gadolinium injections (Omniscan, GE health care, 0.1 mmol/kg body weight).

Image Analysis

To analyze sellar or parasellar tumors on MRI we used the following anatomical approach.

1. First identify the pituitary gland and sella turcica.
2. Then determine the epicentre of the lesion and whether it is in the sella or above, below or lateral to the sella.
3. If it is in the sella, determine whether or not the sella is enlarged.
4. Once the location of the mass is clear, analyze the signal intensity patterns: is the lesion cystic or solid?

A) if solid the signal intensity of mass:
t1w-hypointense/isointense/hyperintense
T2w -hypointense/isointense/hyperintense.

5. Margins of mass: smooth /irregular/sharp.
6. Dural attachment of the mass: widebased /narrow-based.
7. Flow voids, calcifications,
8. Pituitary stalk
9. Chaismatic involvement
10. Cavernous sinus involvement
11. Clival involvement
12. Degree of contrast enhancement: moderate/marked.
13. Contrast enhancement pattern: homogenous/heterogeneous
14. Dural enhancement adjacent to the mass
15. Finally establish a differential diagnosis.

Statistical analysis: Data will be analysed using SPSS 21.0 software. Descriptive parameters will be represented as mean with SD or median. Continuous variables will be compared using unpaired t-test/Mann Whitney u test. Chi-square or t-test will be used to determine significant outcome differences. The agreement between MRI Diagnosis and Histopathological diagnosis will be measured using kappa statistics. Categorical data will be represented as frequency with percentage. For all tests, a p-value of <0.05 will be considered statistically significant.

RESULTS

Out of 20 pituitary adenomas (14 macroadenomas, 6 microadenomas) 3 macroadenomas, 3 microadenomas were functioning. 78.5% of macro adenomas (11) and 50% of microadenomas were non-functioning. The commonest of them was prolactinoma followed by ACTH-secreting adenomas and growth hormone-secreting adenomas. One case was of Nelson syndrome, another of mixed macro adenoma. These patients present with endocrinopathy. Functioning adenomas were more commonly seen in females 7 out of 8.

Micro adenomas (4 – 8 mm) were confined to sella without extension into surrounding structures. On MR imaging 5 out of 6 microadenomas were hypointense on both T1 and T2.

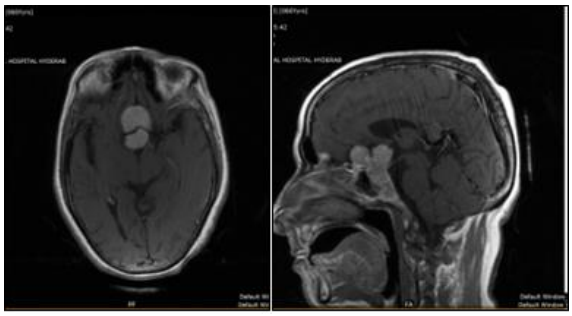

Figure 3: Axial and(c) Sag CEMR T1w images show homogenously enhancing lesions in sella extending superiorly into ant. interhemispheric fissure encasing A1 of both ACAs and ACOM.

Most of the macro adenomas were clinically diagnosed because they presented with visual disturbances or other mass effects. Macro adenomas >1cm causing expansion of sella almost all of them

ISSN (O): 2687-5365; ISSN (P): 2753-6556

showed suprasellar extension, displacing and compressing the optic chaisma. 5 cases had a figure of eight appearances and 6 cases with cavernous sinus invasion. Out of these cases, 3 cases showed encasement of the cavernous segment of ICA, 2 cases showed clival invasion, 1 case showed sphenoid sinus invasion, 1 case showed encasement of both ACAs and ACOM and the same case showed peripheral rim of calcification.

MR imaging of the macroadenomas showed that the majority were homogenous and isointense to grey matter on T1 and hyperintense on T2. Cystic changes were seen in 6 cases and haemorrhage with fluid levels was observed in 1 case.

In all of the microadenomas posterior pituitary bright spot was seen except for one case. In all cases of macroadenoma posterior pituitary bright spot was not identified . 2 cases of macroadenoma turned out to be one of each craniopharyngioma and meningioma histopathologically.

Out of all cases, 5 cases were craniopharyngiomas, with ages ranging from 8 years to 14 years. 3 cases showed a solid cystic mass with calcifications in the suprasellar cistern extending into Sella, one case showed a purely cystic lesion with rim and clumps of calcification, solid components and the periphery of the cysts show rim enhancement. One case of craniopharyngioma was pituitary adenoma on histopathology.

Out of 30 cases, 4 cases were meningiomas aged between 16 years to 57 years with a broad base towards sphenoid. One case shows calcifications. On contrast-enhanced scans, two cases of meningiomas show a dural tail. One case of meningioma was pituitary adenoma on histopathology. 11 cases of pituitary macroadenoma, 4 cases of craniopharyngioma, and 3 meningiomas were operated.

Histologically, meningioma cases showed meningiotheliomatous pattern with cells wrapped in tight whorls with large nuclei and eosinophilic cytoplasm and all were grade I according to the WHO classification. Pituitary adenomas show the following findings: small round cells with monotonous uniform nuclei and eosinophilic cytoplasm. Craniopharyngiomas show adamantinimatous histopathology multistratified squamous epithelium with nuclear palisading, and nodules of "wet" keratin.

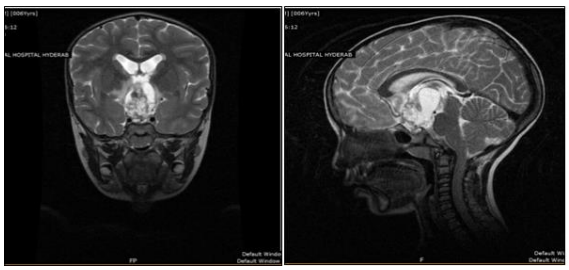

Figure 4: (a)Coronal and (b)Sag T2 images showing a hetergenouslyhyperintense lesion in suprasellar cistern.

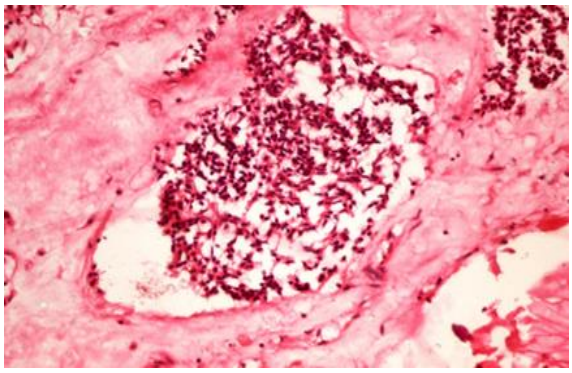

Figure 5: Histopathology shows- Multistratified squamous epithelium with nuclear palisading, nodules of "wet" keratin.

Table 1: Age distribution.

	Age distribution	No of patients
1	1 - 10 yrs	4
2	11 - 30 yrs	10
3	31 - 50 yrs	10
4	51 - 70 yrs	5
5	>70 yrs	1

Table 2: Sex distribution of the study subjects

	Sex	Number of cases	Percentage of cases
1	Males	18	60
2	Females	12	40

Out of 30, 18 were males and 12 were females. Age ranges include from 6yrs to 85 years.

Table 3: Types of lesions

	Types Of Lesions	No. Of Cases
1	Pituitary Adenoma	20
2	Craniopharyngioma	5
3	Meningioma	4
4	Aneurysm	1

The most common tumour observed in the study was 14 cases were pituitary macro adenoma, followed by 6 cases of microadenoma constituting 66.6%, 5 cases were craniopharyngiomas16.6%, 4 meningiomas 13.3% and 1 case was an aneurysm of left supraclinoid ICA diagnosed on MR.

ISSN (O): 2687-5365; ISSN (P): 2753-6556

Table 4: Type of Functioning Adenoma

	Type of Functioning Adenoma	No. Of Patients
1	Prolactinoma	4
2	ACTH Adenoma	2
3	GH Adenoma	1
4	Mixed	1

Table 5: Comparison of MRI diagnosis of Pituitary adenoma, meningioma and craniopharyngioma with Histopathology diagnosis of the study subjects (n=18)

		Histology Diagnosis			Total
		Pituitary Adenoma	Adamantinomatus type of Craniopharyngioma	Meningiotheliomatous Meningioma	
MRI Diagnosis	Macroadenoma	9	1	1	11
	Craniopharyngioma	1	3	0	4
	Meningioma	1	0	2	3
Total		11	4	3	18

Table 6 (a): MRI diagnosis Vs HPE of the pituitary adenomas

		Histopathology		
		Pituitary Adenoma	Non-Pituitary adenoma	Total
MRI	Macroadenoma	9	2	11
	Non Macroadenoma	2	5	7
	Total	11	7	18

Table 6 (b): Comparison of MRI diagnosis of Macro adenoma with Histopathology diagnosis of the study subjects (n=11)

Sensitivity	81.8%
Specificity	71.4%
Positive predictive value	81.8%
Negative predictive value	71.4%
Per cent agreement	77.8%
Kappa value	0.532
P value	0.024

The sensitivity of MRI diagnosis of Macroadenoma compared with histopathology is 81.8% and its specificity is 71.4%. The positive predictive value for MRI diagnosis of Macroadenoma compared with histopathology is 81.8% and its Negative predictive value is 71.4%. The per cent agreement for comparison of MRI diagnosis of Macroadenoma compared with histopathology is 77.8% and positive per cent agreement is 81.8%. When kappa statistics is applied the kappa value is 0.532, this shows moderate agreement between the MRI Diagnosis and Histopathological diagnosis of Macroadenoma with the statistically significant p-value 0.024.

Table 7(a): MRI Vs HPE in craniopharyngiomas

		Histopathology		
		Adamantinomatous type of Craniopharyngioma	Non-Adamantinomatous type of Craniopharyngioma	Total
MRI	Craniopharyngioma	3	1	4
	Non-Craniopharyngioma	1	13	14
	Total	4	14	18

Table 7(b): Comparison of MRI diagnosis of Craniopharyngioma with Histopathology diagnosis of the study subjects (n=18)

Sensitivity	75%
Specificity	92.8%
Positive predictive value	75%
Negative predictive value	92.8%
Per cent agreement	88.9%
Kappa value	0.679
P value	0.004

The sensitivity of MRI diagnosis of Craniopharyngioma compared with histopathology is 75% and its specificity is 92.8%. The positive predictive value for MRI diagnosis of Craniopharyngioma compared with histopathology is 75% and its Negative predictive value is 92.8%. The per cent agreement for comparison of MRI diagnosis of Craniopharyngioma compared with histopathology is 88.9% and positive per cent agreement is 75%. When kappa statistics is applied the kappa value is 0.679, this shows substantial agreement between the MRI Diagnosis and Histopathological diagnosis of Macroadenoma with the statistically significant p-value of 0.004.

ISSN (O): 2687-5365; ISSN (P): 2753-6556

Table 8(a): MRI vs HPE in diagnosing meningioma

		Histopathology		
		Meningiotheliomatous Meningioma	**Non-Meningiotheliomatous Meningioma**	**Total**
MRI	Meningioma	2	1	3
	Non-Meningioma	1	14	15
	Total	3	15	18

Table 8(b): Comparison of MRI diagnosis of Meningioma with Histopathology diagnosis of the study subjects (n=18)

Sensitivity	**66.7%**
Specificity	93.3%
Positive predictive value	66.7%
Negative predictive value	93.3%
Per cent agreement	88.9%
Kappa value	0.600
P value	0.011

The sensitivity of MRI diagnosis of Meningioma compared with histopathology is 66.7% and its specificity is 93.3%. The positive predictive value for MRI diagnosis of Meningioma compared with histopathology is 66.7% and its Negative predictive value is 93.3%. The per cent agreement for comparison of MRI diagnosis of Macroadenoma compared with histopathology is 88.9% and positive per cent agreement is 66.7%. When kappa statistics is applied the kappa value is 0.600, this shows moderate agreement between the MRI Diagnosis and Histopathological diagnosis of Meningioma with the statistically significant p-value 0.011.

DISCUSSION

The sellar/para sellar and suprasellar region is an anatomically complex area with a variety of pathological lesions both neoplastic and non-neoplastic lesions occurring in this confined space and require a combination of endocrinologic, ophthalmic and neurological examinations along with advanced neuroimaging modalities.

The study included 30 patients with a clinical diagnosis of pituitary adenomas, suspicious of pituitary adenomas, intracranial space-occupying lesions and to rule out CSVT were included in the study. Sellar and parasellar tumours were analysed based on clinical findings, laboratory investigations and MR imaging. Tissue diagnosis (Biopsy) after surgery was done in feasible cases and tissue diagnosis was given in them.

MRI is the gold standard imaging modality to characterise such lesions due to superior soft tissue contrast differentiation, availability of advanced sequences offering high spatial resolution and nonexistence of ionising radiation, thus allowing accurate visualisation of mass effects on neighbouring soft tissues.

Pituitary adenoma: In our study, the commonest tumour was pituitary adenomas, to be specific macroadenomas constituted about 46.6% of the cases, and 20% of cases were microadenomas together constituting 66.6%. 16.6% were craniopharyngiomas, and 13.3% were meningiomas, of all the sellar and parasellar tumours. The percentage of pituitary adenoma in our study was similar to that seen in a study by Awatif A (65.45%).[9] Batra V et al,[10] concluded that females predominate (60%,) with pituitary adenoma in their study. Banna et al,[11] had a similar finding in their study which is a female preponderance. But, Awatif et al9 had noted male preponderance in pituitary adenomas. The percentage of males and females with pituitary adenoma in our study results were similar to that in Awatif et al.[9] Macroadenomas were the commonest tumours of pituitary adenomas in imaging studies (70%) and microadenomas were 30%. The results were closer to those of Sweta Da Silva Pereira et al,[12] which had macro adenoma forming 62.5%.

Normal pituitary parenchyma shows homogenous enhancement at 60-80ms following the administration of contrast. Maximum image contrast can be seen at about 1 minute and gradually decreases thereafter. However, an adenoma may be enhanced earlier than pituitary tissue due to direct arterial supply. We, in our study, noted that most of the macroadenomas homogenously enhanced on contrast MRI and heterogenous in a few cases with haemorrhage. The findings were in concordance with those in a study by Batra et al,[10] and Hui et al.[13] Batra et al,[10] noted 70% of macroadenomas showed homogenous contrast enhancement. So did Hui et al,[13] where 71% of macroadenomas with homogenous enhancement. Sweta Da Silva Pereira et al,[12] noticed that 60.4% were homogenous amongst the macroadenomas.

The coronal section helps in the assessment of suprasellar extension of the lesions. Sagittal images were used to localise the lesion. T2w, DWI, and ADC imaging help in the assessment of the consistency of the lesion, soft lesions are hyperintense on T2, hard lesions are hypointense on T2, softer the lesion higher the ADC values. The pulse sequence for best tissue contrast and anatomic display in this region is generally accepted to be T1-weighted imaging because the characterization of components of the lesion was easy on T1. While signal intensity on T2 weighted images is variable due to haemorrhage, cystic nature or necrosis. In our study 10 macroadenomas were isointense on both T1 and T2,

ISSN (O): 2687-5365; ISSN (P): 2753-6556

3 cases were isointense on T1 but hyperintense on T2 and 2 cases were hypointense on both T1 and T2. Hui et al,[13] also noticed similar findings of 85% of T1 were isointense but hyperintense on T2 signals. Batra V et al,[10] and Johnsen et al,[14] had similar findings of 82% isointense and 18% hyperintense on T1 signals. Sweta Da Silva et al,[12] published that 60.3% of macroadenomas appeared isointense on both T1W and T2W. In 7.5% of cases, it was hypointense on T1 and hyperintense on T2.

Up to 10% of macroadenomas invade the cavernous sinuses and tend to be biologically aggressive, with increased surgical morbidity and mortality. Imaging features that may be indicative of cavernous sinus invasion are usually assessed on the coronal pre and post-contrast T1 weighted images. Cottier et al,[15] considered 67% encasement of the internal carotid artery by the tumour as it had 100% positive predictive value. Obliteration of the carotid sulcus venous compartment and tumour extension beyond the lateral intercarotid line are some other features. Criteria followed in our study to describe cavernous sinus invasion are asymmetry of cavernous sinuses, encasement of ICA> 45%, presence of adenoma lateral to ICA, and bulging of the lateral wall of the cavernous sinus.

Of all the macroadenomas studied 5 cases showed cystic changes, 4 cases showed cavernous sinus invasion, 3 cases showed encasement of cavernous segment of ICA, 1 case showed clival invasion, 1 case showed sphenoid sinus invasion, and only 6 cases were microadenomas with pure sellar location.

Meningiomas arise from arachnoid cap cells in the leptomeninges, which derive from the mesenchyme and neural crest. They are almost always dural-based and commonly along dural reflections. In the anterior skull, it can arise from sphenoid wings, tuberculum sellae, limbus sphenoidal, and chiasmatic and olfactory grooves. on MRI, they are usually well-circumscribed, iso to hypointense on T2, and show avid contrast enhancement. Although not specific, identification of a dural tail may suggest a meningioma if: (a)the tail is thick and closer to the tumour and taper peripherally, (b) enhanced to a greater degree than the tumour, (c) the tail must be seen in two consecutive sections in more than one plane. The majority of the 3 cases (12% of sellar and parasellar tumours) reported in the current study were in para-sellar locations and were sphenoid meningiomas with meningiotheliomatous patterns and extending into suprasellar and Sella, all of them were grade I by WHO classification system. One case showed calcifications within. All cases of meningiomas showed homogenous enhancement. Classical features like dural tail were seen in two cases. Hyperostosis was not seen in any of the cases. In all these cases pituitary function was normal. Patients presented with headaches and visual disturbances.

Craniopharyngiomas have no gender predominance but with bimodal age distribution and a peak incidence rate in children and adults between 5-14 and 50-74 years respectively. In our study, most cases are of paediatric age group < 14 years, only one case was a 33-year-old. In our study, they account for 20 % out of all sellar/ parasellar lesions with adamantinomatous histological patterns and presented clinically with visual disturbance and increased intracranial pressure. In the current study, all the craniopharyngioma were located in the suprasellar cistern extending into sella and parasellar areas. In craniopharyngiomas, better characterization of lesions was seen on MRI. All cases are solid and cystic with calcified foci enhancement of the solid area of the lesion and periphery of the cyst seen. Two cases showed recurrence within one year of duration.

CONCLUSION

The MR imaging properties of the four most prevalent lesions were distinct enough to distinguish them from one other and the majority of other entities. Other imaging characteristics, such as augmentation post-contrast, the presence of cystic components, extracellular and intrasellar placement, and clinical complaints, allow for additional separation among the various other abnormalities. MR imaging's better resolution and multiplanar capability best display the extent of sellar and parasellar lesions.

REFERENCES

1. Anna Derman MD, Marisa Shields, Adam Davis MD, Edmond Knopp MD, Girish M Fatterpekar MBBS. Diseases of the Sella and Parasellar Region: An Overview. Seminars in roentgenology 2013, 35-50.
2. De Herder WW. The History of Acromegaly. Vol. 103, Neuroendocrinology 2016, p. 7-17.
3. Herder WW. Acromegaly and gigantism in the medical literature. Case descriptions in the era before and the early years after the initial publication of Pierre Marie (1886). Pituitary 2009;12(3):236-44.
4. Swartz JD, Russell KB, Basile BA, O'Donnell PC, Poply GL. High-resolution computed tomographic appearance of the intrasellar content in women of childbearing age. Radiology 1983; 147:115-117.
5. Sartor K, Karnaze MG, Winthrop JD, Gado M, Hodges FJ. MR imaging in infra-, para- and retrosellar mass lesions. Neuroradiology 1987;29(1):19-29.
6. Lee BCP, Kneeland JB, Walker RW, Posner JB, Cahill PT, Deck MD, et al. MR imaging of brainstem tumours. Am J Neuroradiol 1985;6(2):159-63.
7. Davis PC, Hoffman JC, Malko JA, Tindall GT, Takei Y, Avruch L, et al. Gadolinium-DTPA and MR imaging of pituitary adenoma: a preliminary report. Am J Neuroradiol. 1987;8(5):8170-23.
8. Brauner R, Argyropoulou M, Perignon F, Rappaport R, Brunelle F. [Role of magnetic resonance imaging in non-neoplastic hypothalamo-hypophyseal pathology]. Ann Pediatr (Paris) 1993;40(7):469-74.
9. Awatif A. Jamal and Rana A. Ajabnoor. Sellar and Parasellar Lesions: A 15-year University Hospital Experience, Saudi Arabia. J Am Sci. 2012; 8(5):74-82]. (ISSN: 1545-1003)
10. Batra V et al.Radiopathological correlation of sellar and suprasellar masses: our experience. Int J Res Med Sci. 2016 Sep;4(9):3924-3928.
11. Bradley G, Schmidt PG Ph.D. Effect of Methemoglobin on the MR Appearance of Subarachnoid hemorrhage. Radiology 1985;156:99-103.

ISSN (O): 2687-5365; ISSN (P): 2753-6556

12. Sweta Da Silva Pereira et al., Magnetic Resonance Imaging in Evaluation of Pituitary Adenomas: International Journal of Anatomy, Radiology and Surgery. 2016 Jul, Vol-5(3): RO01-RO05.
13. Hui P, Parida S, Mohanty J, Singh M, Sarangi PK. Accuracy of magnetic resonance imaging in evaluation of sellar juxtasellar tumors. Oncol J India 2019; 3:3-9.
14. Johnson MR, Hoare RD, Cox T, Dawson JM, Maccabe JJ, Llewelyn DE, McGregor AM.The evaluation of patients with a suspected pituitary microadenoma: computer tomography compared to magnetic resonance imaging.Clin Endocrinol (Oxf). 1992 Apr;36(4):335-8.
15. Scotti G, Yu CY, Dillon WP, Norman D, Colombo N, Newton TH, et al. MR imaging of cavernous sinus involvement by pituitary adenomas. Vol. 9, American Journal of Neuroradiology 1988, p. 657-64.

ISSN (O): 2687-5365; ISSN (P): 2753-6556